Original Article

The Effect of Different Core/Veneer Thickness Ratios on Stress Distribution of Implant-supported Zirconia-ceramic Posterior Crowns: A 3-D Finite Element Analysis

Hui-Ling Chen, DDS, MS
Department of Dentistry National Yang-Ming University, Taipei, Taiwan

Chih-Ling Chang, DDS, MS, PhD
Assistant Professor, School of Dentistry National Yang-Ming University, Taipei, Taiwan
Director and Chief, Dental Department Shin Kong Wu Ho-Su Memorial Hospital, Taipei, Taiwan

Chen-Sheng Chen, DDS, MS, PhD
Department of Physical Therapy and Assistive Technology, National Yang-Ming University, Taipei, Taiwan

Ling-Ming Yu, DDS
Attending doctor, Department of Dentistry, Chang-Gung Memorial Hospital, Taipei, Taiwan

Ming-Lun Hsu, DDS, MS, PhD
Dean, School of Dentistry National Yang-Ming University, Taipei, Taiwan

Corresponding author:
Ming-Lun Hsu, DDS, MS, PhD
National Yang-Ming University
No.155, Linong St., Beitou Dist.,
Taipei City 11221, Taiwan R.O.C.
Tel: +886-2-2821-2943
E-mail: mlhsu@ym.edu.tw

Abstract

Purpose

To evaluate the effect of different core/veneer thickness ratios on stress distribution in implant-supported zirconia-ceramic posterior crowns.

Material and methods

Nonlinear contact finite element analysis was used to evaluate the stress distribution in zirconia-ceramic crowns under axial and oblique loading. Implant-supported maxillary first molar crowns with an occlusal thickness of 3 mm were constructed. Five models with the following different core/veneer thickness ratios were used: model I – 1/5 (0.5 mm/ 2.5 mm), model II – 1/2 (1 mm/ 2 mm), model III – 1/1 (1.5 mm/ 1.5 mm), model IV – 2/1 (2 mm/ 1 mm), and model V – 5/1 (2.5 mm/ 0.5 mm). The 1st principal stress and von Mises stress were analyzed to observe the effect of different core/veneer thickness ratios on the stress distribution.

Results

Whether under axial loading or oblique loading, the different core/veneer thickness ratios only affected the stress distribution in the core and veneer layer. The 1st principal stress results showed that the stress dissipation decreased as the core/veneer thickness ratio increased. The stress generated by oblique loading was greater than that generated by axial loading. Under axial loading, model V showed a higher maximum von Mises stress magnitude, but other models had no significant difference. As for oblique loading, model V also showed a higher maximum von Mises stress magnitude. Furthermore, model III and model IV revealed relatively favorable stress magnitudes in comparison with the other models.

Conclusion

The different core/veneer thickness ratios of the zirconia-ceramic crowns influenced the stress distribution on the crowns but not the implant component or supporting bone structures. Under axial loading, the core/veneer thickness ratio of 5/1 was unfavorable in terms of stress distribution. Meanwhile, the core/veneer thickness ratios of 1/5, 1/2, 1/1, and 2/1 showed no obvious differences with one another. As for oblique loading, the core/veneer thickness ratios of 1/1 and 2/1 were relatively favorable for stress distribution.

Keywards: core/veneer thickness ratio, finite element analysis, zirconia-ceramic restorations

Introduction

The current trend in prosthetic dentistry leads to metal-free restorations. The advances in CAD (computer-aided design)/CAM (computer-aided manufacturing) technology have enabled the frequent use of these high strength ceramic restorations in dentistry, especially those containing zirconia[1]. Zirconia had been used to make posts and cores, orthodontic brackets, frameworks for all-ceramic restorations, implant fixtures, and implant abutments[2]. As the core material for all-ceramic restorations, the opacity restrained the esthetic outcome compared to other all-ceramic systems. Therefore, the application of veneer porcelain over a zirconia core is often necessary to improve the esthetics of restoration containing zirconia. Such zirconia-ceramic restorations have become increasingly popular in the last few decades.

According to a literature review of the relevant clinical studies, the survival rates of zirconia-ceramic restorations consisting of either single crowns or fixed dental prostheses seem to be comparable to those of metal-ceramic restorations. However, the cohesive failure (that is, chipping) of porcelain veneers was identified as the most intractable technical problem affecting such zirconia-ceramic restorations[3, 4]. Relatedly, implant-supported zirconia-ceramic restorations have been found to exhibit significantly higher veneer chipping rates than implant-supported metal-ceramic restorations[1, 5, 6, 7].

The causes of veneer chipping are still uncertain. Many factors have been suspected of being associated with veneer chipping. These factors include the bond strength between the zirconia core and the porcelain veneer, residual thermal stress, occlusal wear damage, the crown geometry (that is, the framework design and relative thickness), and the material of the porcelain veneer, among others[1, 3, 8]. It is believed that veneer chipping is a multifactorial phenomenon.

The crown geometry including the framework design and relative core/veneer thickness is one parameter that dentists can control. Since the optimization of the zirconia cores used in zirconia-ceramic restorations with anatomically supported designs has been proven to reduce veneer chipping[9, 10], there is some question as whether the design of the relative thickness in the zirconia-ceramic restorations could affect their clinical performance. Several in vitro studies have shown that different core and veneer thicknesses in zirconia-ceramic restorations have an influence on their hardness, fracture resistance, fracture toughness, and residual stress[11, 12, 13, 14, 15].

Esquivel-Upshaw et al.[16] evaluated several design parameters including core/veneer thickness ratios, gingival connector embrasure designs, and the connector heights of implant-supported zirconia-ceramic and metal-ceramic fixed dental prostheses in a randomized clinical trial. Although no significant associations were reported between these parameters and the survival probability, it was noted that zirconia-ceramic prostheses exhibited more chipping failures with a core/veneer thickness ratio of 1/1, whereas metal-ceramic prostheses exhibited more chipping failures with a core/veneer thickness ratio of 1/3. Such differences have generated interest in exploring this issue further.

Several studies have used finite element analysis to evaluate the influence of different design parameters, especially framework designs, on stress distribution in crown restorations[17, 18, 19, 20, 21]. Anami et al.[19] reported that the geometry and design could affect the stress distribution of zirconia-ceramic crowns. Their study also indicated that the dimensions of the core and veneer layer could result in differences in stress values.

Pross et al.[22] evaluated the effect of veneer layer thickness on stress distribution by using a two-dimensional axisymmetric model of In-Ceram anterior bridges. With veneer layer thicknesses ranging from 0 mm to 1.6 mm, the maximum tensile stress at the bridge surface varied. The lowest maximum tensile stress occurred with a veneer thickness of 0.4 mm. Moreover, when the veneer layer thickness was less than 0.2 mm or greater than 1 mm, the maximum tensile stress exceeded the yield strength of the veneer porcelain. This indicated that an optimal core/veneer thickness ratio might exist to minimize the stress magnitude and reduce veneer fracture.

Furthermore, Anusavice et al.[23] reported that the different core/veneer thickness ratios and load orientations in bilayered lithium-disilicate-based ceramic crowns have an impact on their time-dependent fracture probability. As the core/veneer thickness ratio was increased, the time-dependent fracture probability decreased. These studies indicated that core/veneer thickness ratios could have an influence on the stress fields affecting all-ceramic restorations.

However, little information regarding the effects of individual designs of different core/veneer thickness ratios on stress distribution in zirconia-ceramic crowns has been made available. Thus, the purpose of this study was to use finite element analysis to evaluate the effect of different core/veneer thickness ratios on stress distribution in implant-supported zirconia-ceramic posterior crowns.

Material and methods

ANSYS software (ANSYS 14.5, ANSYS, Canonsburg, PA, USA) was used to generate the three-

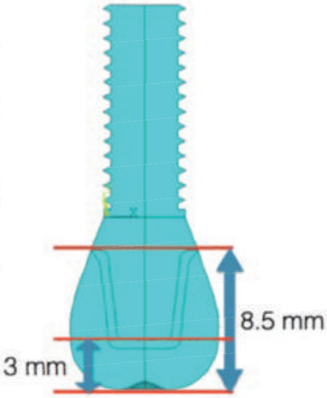

Fig 1. Dimensions of zirconia-ceramic crown

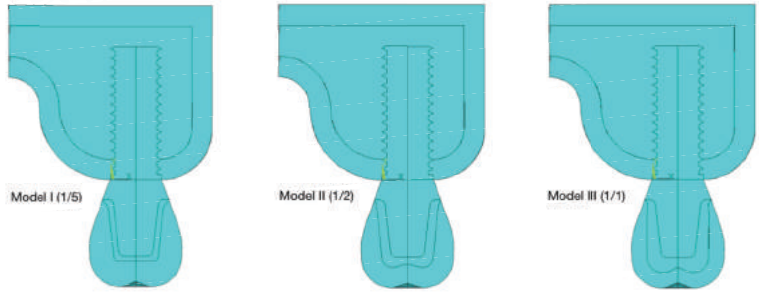

Model	I	II	III	IV	V
Core (mm)	0.5	1	1.5	2	2.5
Veneer (mm)	2.5	2	1.5	1	0.5
Core/veneer thickness ratio	1/5	1/2	1/1	2/1	5/1

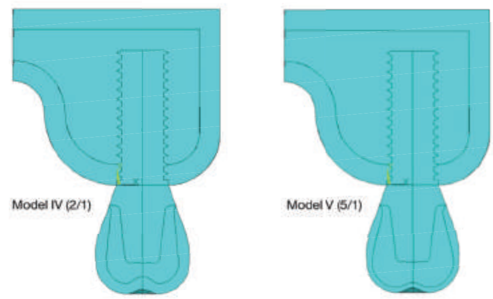

Fig 2. Cross-sectional views of the five investigated models

dimensional models, create the mesh of individual elements, and generate the post-processing data needed to calculate the stress of each model. Each model included an implant, abutment, crown, antagonist tooth, and the relevant section of maxillary bone. A maxillary molar was used as a reference to construct the crown.

The geometry of the 13-mm 3i Full OSSEOTITE® Certain® implant (3i, Implant Innovations Inc. Fluoride, U.S.A) was used as a reference to construct the model. The implant was 5 mm in diameter and 13 mm in total length. The abutment was 7.5 mm in height with a 2 mm collar height, and the emergence profile was 6.5 mm. For convenience in terms of the model construction, the anatomic shape of the maxillary molar was simplified. The overall dimensions of the zirconia-ceramic crown from the margin of the abutment to the top of the crown was 8.5 mm in height and 9 mm in width (Fig. 1). The thickness of the crown was 3 mm at the occlusal surface. Five models with different core thicknesses and veneer layer thicknesses in the cusp area were constructed, but all the models were the same in terms of their outer shape (Fig. 2). Specifically, five models with the following different core/veneer thickness ratios were used: model I – 1/5, model II – 1/2, model III – 1/1, model IV – 2/1, and model V – 5/1.

The bone-implant interface was assumed to be completely osseointegrated. In addition, the interfaces between the veneer layer, core layer, abutment, and implant were all assumed to be perfectly bonded. The material properties of all the materials were known from the literature[21, 24, 25]. The cortical and cancellous bones were considered to be homogenous, anisotropic, and linearly elastic. The implant, abutment, zirconia-ceramic crown, and opposite tooth were also considered to be homogeneous, isotropic, and linearly elastic in the model. All the mechanical properties of the materials are listed in Table 1.

Material	Young's modulus (MPa)		Poisson ratio	Reference
Implant & abutment (Titanium)	110,000		0.35	Chang CL et al.[24]
Core (zirconia)	210,000		0.3	Chang CL et al.[24]
Veneer (porcelain)	65,000		0.23	Sung M et al.[21]
Cortical bone	Ex 17900 Ey 12500 Ez 26600	Gyx 4500 Gyz 5300 Gxz 7100	v_{yx}0.18 v_{yz}0.31 v_{xz}0.28	Chang CL et al.[24]
Cancellous bone	Ex 1148 Ey 21 Ez 1148	Gyx 68 Gyz 68 Gxz 434	v_{yx}0.055 v_{yz}0.055 v_{xz}0.322	Chang CL et al[24]
Enamel	84,100		0.33	Dejak B et al.[25]

Table 1. Mechanical properties of the materials

The 10-node tetrahedral solid 187 element and 4-node shell 181 element were used in the study. The pairs of contact elements (target 170 and contact 174) were used at the occlusal surface of each examined crown and opposite tooth. The coefficient of friction between the contact surfaces was assumed to be 0.2[25]. The models were constrained on all nodes of the mesial and distal external surfaces of bone segment in all directions.

The contact analysis method was used in this study, and two different loading conditions were assumed. Both axial loading and oblique loading were applied a motion to maximal intercuspal position. For the axial loading, the nodes on the bottom of the opposite tooth were moved along the y-axis until a reaction force of 300N was achieved. As for the oblique loading, the nodes on the bottom of the opposite tooth were applied along the x-axis and y-axis to produce a reaction force of 350N. The contact simulation of the FEA entailed a nonlinear analysis that required the load and displacement to be applied in a number of steps. Automatic time stepping was applied in this analysis.

The contour plots of the stress distribution, including von Mises stress and the 1st principal stress (tensile stress), were used to compare the different models. The values of the maximum von Mises stress and maximum 1st principal stress for each model were utilized in histograms in order to compare the models.

Results

The accuracy of the model was verified by convergence test. The elements of all the models investigated in the study were between 88993 and 100567. As for the nodes, they were all between 115060 and 130614.

Results of axial loading

The pattern of stress distribution among the five models was similar (Fig. 3). The maximum von Mises stress values applied to the cortical bone, cancellous bone, and implant did not differ significantly. For model V, however, the peak von Mises stress values in the veneer and core layer were significantly greater than those for the other models.

In the veneer layer, the 1st principal stress was localized around the contact area in all five models. When viewed as a cross-section, it could be seen that the 1st principal stress was more dispersed in model I compared to the other four models. As for the core layer, stress concentration beneath the contact areas was more obvious as the core/veneer thickness ratio increased. The peak value in model V was greater than those in the other models (Figs. 4, 5).

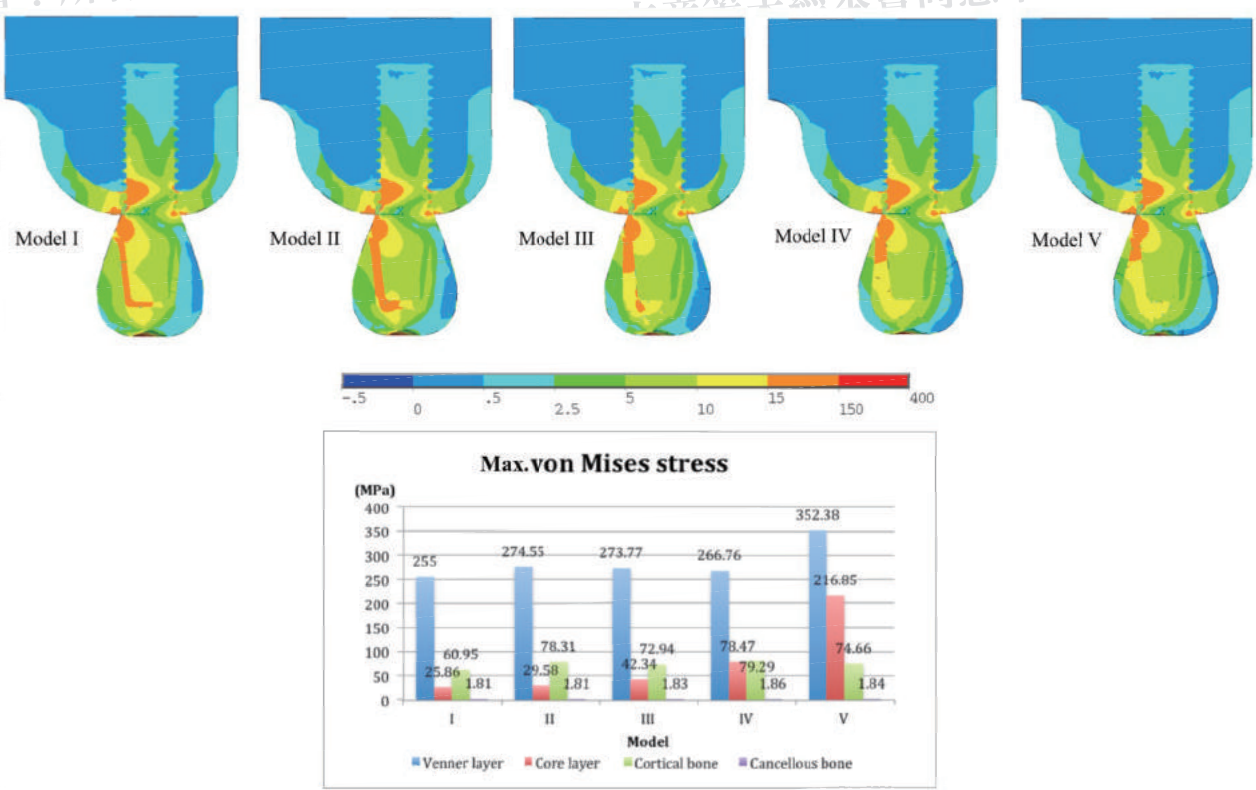

Fig 3. Axial loading—von Mises stress of main model and maximum value

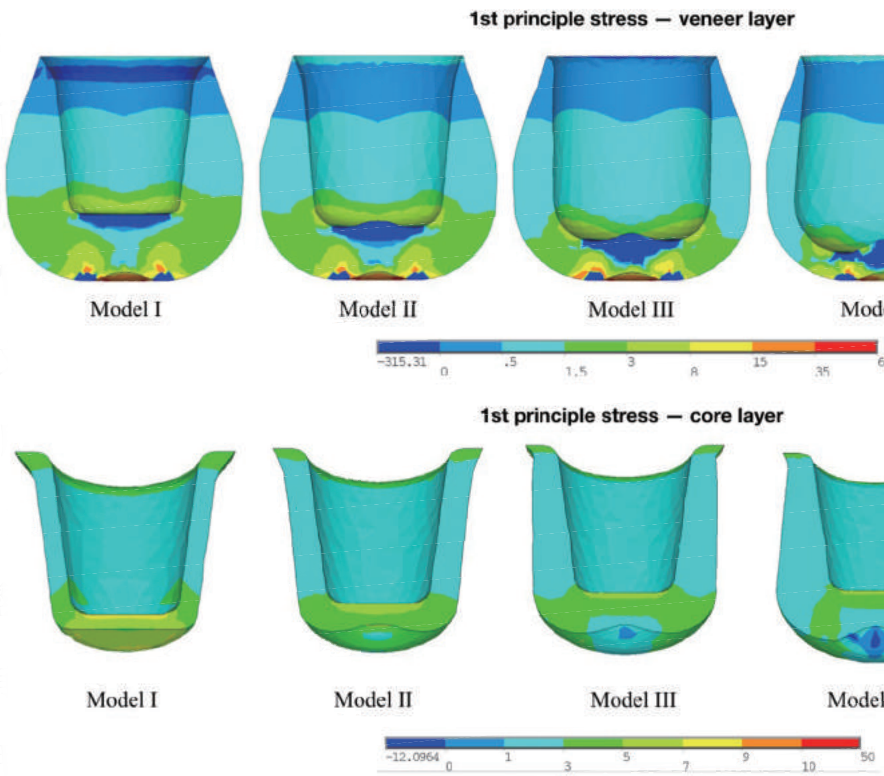

Fig 4. Axial loading—1st principal stress in the core and veneer layer

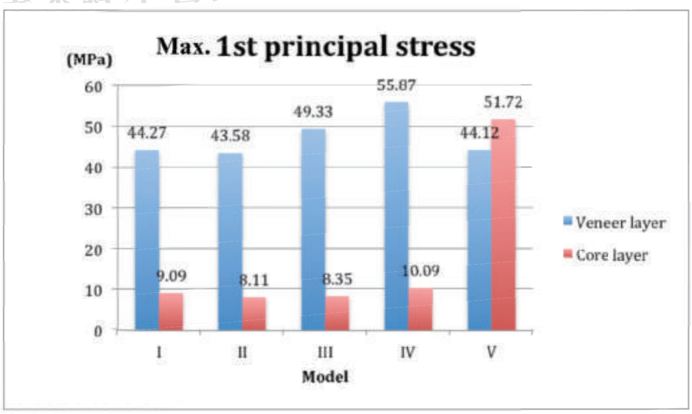

Fig 5. Axial loading—maximum 1st principal stress in the core and veneer layer

Results of oblique loading

The pattern of von Mises stress was similar in all five models (Fig. 6). In model V, both the veneer layer and core layer had significantly greater peak values than the other models. In addition, the peak value of the veneer layer was lower in model III and model IV.

The maximum 1st principal stress in the veneer layer was also located around the contact area in all five models. From the cross-sectional view, it could be seen that compressive stress was concentrated in the contact area and the veneer core interface beneath it. The peak value was greatest in model I and slightly decreased as the veneer thickness decreased. The maximum 1st principal stress in the core layer was located at the cervical margin opposite to the loading direction. The peak value of the maximum 1st principal stress in the core layer of model V was significantly greater than that in the other models (Figs. 7, 8).

Discussion

It is well known that ceramic material is less resistant to tensile stress[17]. With a finite element analysis, it is possible to determine from the stress concentration areas where a

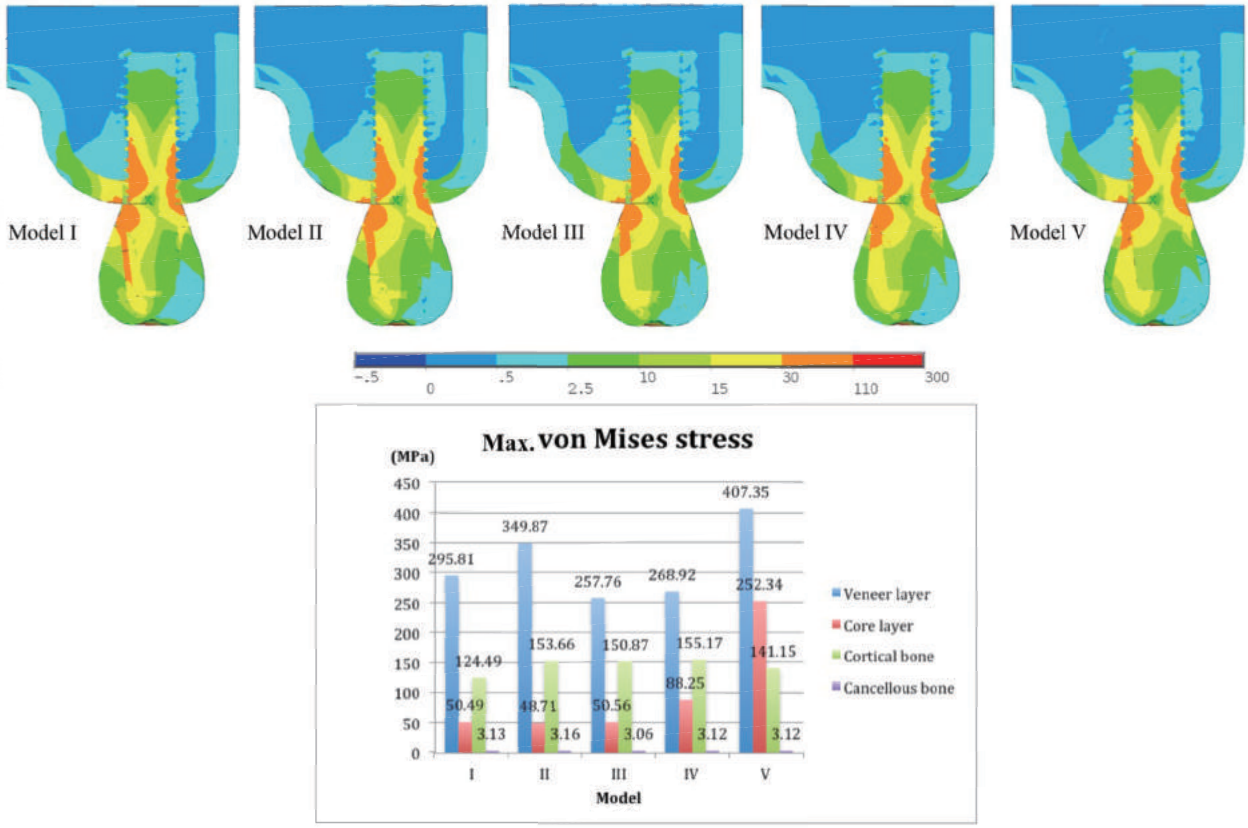

Fig 6. Oblique loading—von Mises stress of main model and maximum value

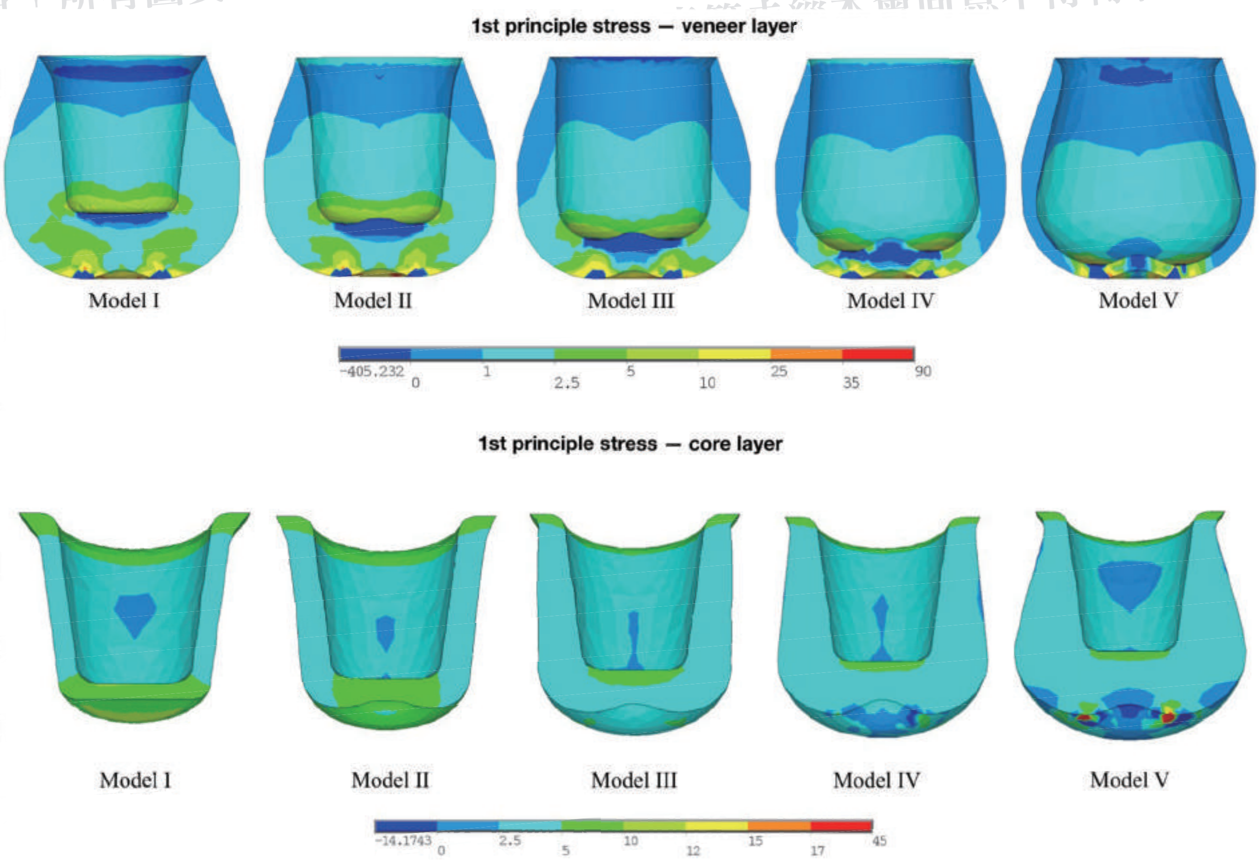

Fig 7. Oblique loading—1st principal stress in the core and veneer layer

fracture could begin. Therefore, the finite element method was used in the present study to provide information that could potentially be used to improve crown designs.

The loading conditions of a finite element model have certain effects on the stress distribution pattern. Previous studies have mostly used linear elastic models, such as those in which force is applied onto a node or an element or pressure is applied onto an occlusal surface to simulate occlusal loading. The above loading condition will lead to excessively concentrated stress peripherally around the loading site[26, 27]. Consequently, it is necessary to remove the singularity during the post processing. In the current study, the purpose was to evaluate the stress distribution patterns in the investigated crowns. However, the fractographic analysis of clinical failed restorations indicated that the fractures mostly originated from the occlusal contact area. As such, it can be concluded that using a linear elastic model may lead to erroneous interpretations of stress distribution patterns in a crown surface. In the studies of Dejak B et al.[25], a cuboid bolus was used to simulate the clinical situation. Nevertheless, the veneer porcelain at the occlusal surface of the crown will be in contact with the opposing dentition during chewing. Consequently the masticatory stress generated during chewing is directly applied on the veneer porcelain in the occlusal region. Thus, contact analysis was used in current study but a food bolus was not simulated.

Since the first molar is located at the center of occlusal loading and withstands the greatest amount of occlusal force, a maxillary first molar was constructed to evaluate the stress state. The human molar bite force ranges from 176N to 750N[28]. In the current study, the axial loading and oblique loading were 300N and 350N, respectively, values which are within the range of normal bite force. In addition, the maximum intercuspation contacts have previously been reported to be significantly associated with the fracture of implant-supported prostheses[29]. Thus, maximum intercuspation contact was assumed in the present study.

In the current study, the von Mises stress magnitude in the supporting bone structures under oblique loading was greater than under axial loading. This result was in accordance with the findings of a previous study[30], which indicated that the oblique load could lead to unfavorable stress concentrations in supporting bone substructures. Therefore, the establishment of an occlusal scheme to reduce lateral occlusal force is recommended in implant-supported restorations.

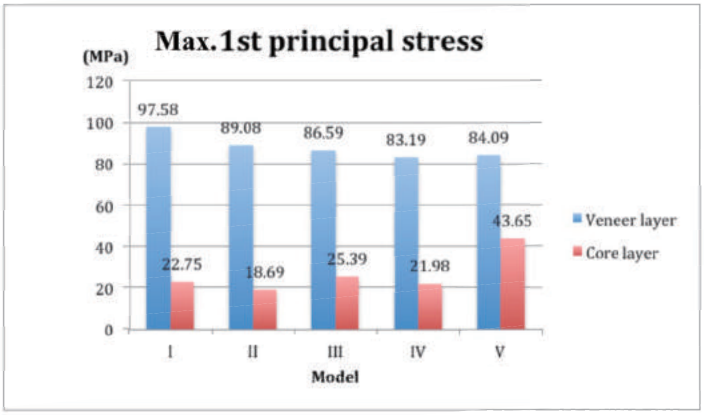

Fig 8. Oblique loading—maximum 1st principal stress in the core and veneer layer

Under axial loading, the maximum 1st principal stress in the core layer significantly increased in model V, although there was no significant difference in the veneer layer. Moreover, from the cross-sectional view it was obvious that the compression stress was concentrated along the contact area and continued to the underlying core layer. This indicated that the veneer layer could not dissipate stress and thus led to significantly increased stress magnitude in the core layer compared to the other four models. This situation was particular obvious in model V with respect to the von Mises stress fields. This indicated that model V, with its core/veneer thickness ratio of 5/1, might undergo the most unfavorable conditions in terms of stress distribution under axial loading.

As for oblique loading, the greatest maximum 1st principal stress in the core layer was also exhibited in model V, just as with axial loading. However, in the veneer layer, model I exhibited the greatest stress magnitude of all the models. Meanwhile, model V had significantly higher maximum von Mises stress values in the core and veneer layer than the other models. In contrast, model III and model IV had lower stress magnitudes. This indicated that the core/veneer thicknesses of 1/1 and 2/1 were more favorable designs under oblique loading.

From the cross-sectional view of the 1st principal stress distribution in crown, it was observed that as the core/veneer thickness ratio was increased, the stress was more concentrated in either loading condition. Meanwhile, although the stiffer zirconia core could assist in allowing the stress to dissipate, the concentrated stress was nonetheless apparent in model V, which had the thinnest veneer thickness compared to the other models. Such stress concentration could lead to the initiation of fractures in the veneer porcelain.

In the present study, the cement layer was not simulated. Rekow et al.[31] evaluated the relative contributions of the variables in a crown-cement-tooth system that can influence the magnitude of maximum principal stress in all-ceramic crowns. Those variables included the crown material, geometry (thickness and cuspal incline), cement modulus and thickness, supporting tooth core, and occlusal loading position. The results of the study showed that the crown material and thickness are of primary importance in stress magnitude. Meanwhile, a study by Kurtoflu C et al.[32] showed that cement thickness had a minor influence on the maximum stress value in ceramic-cement-dentin multilayer systems. However, the ceramic type and thickness had significant impacts on the maximum principal stress value. Wimmer T et al.[33] also found that the Young's modulus of the cement layer only affected the maximum principal stress values in the cement layer. In addition, neither the Young's modulus nor the thickness of the cement layer influenced the displacement and stress distribution of prostheses. Shahrbaf et al.[34] also reported that the elastic modulus of cement did not affect the stress state in the crown and supporting structure of a crown-tooth system. Meanwhile, because the purpose of the current study was to evaluate the individual effect of different core/veneer thickness ratios, the cement layer was negligible.

In the process of zirconia-ceramic restorations, a mismatch of the thermal expansion coefficient and the thermal gradient of cooling will lead to the development of residual stress. Such residual stress could lead to unstable cracking or chipping of porcelain veneer. Swain et al.[35] used a mathematical model to determine that a thicker veneer layer on a zirconia core will generate higher residual stress. Guazzato et al.[36] also pointed out that spontaneous cracking in porcelain/zirconia structures increases with increasing veneer layer thickness. In addition, studies have reported that the magnitude of residual stress is increased with increased veneer layer thickness[37, 38]. However, the effect of residual stress was not taken into account in the present study. Thus, the maximum stress values observed in this study should not be directly compared with other laboratory results; rather, the results in this study should only be compared with each other.

Only a convergence test was conducted to verify the accuracy of the finite element model used in the current study. However, further in vitro validation of the finite element model will improve its reliability and could allow for direct comparison with the results of other studies.

In the current study, a total occlusal thickness of 3 mm was used in five different core/veneer thickness ratios to evaluate the stress distribution pattern under mechanical loading. A further study will be aimed at investigating the effects of other total occlusal thicknesses, such as 2 mm, as well as other restoration materials. In addition, the interactions between thermal residual stress and the core/veneer thickness ratios should be taken into consideration to provide clinicians with more reliable design guidelines in making crown restorations.

Conclusion

The limitations of the present study notwithstanding, the following conclusions were reached:

1. The different core/veneer thickness ratios of zirconia-ceramic crowns have an influence on the stress distributions in such crowns but not on the stress distributions of the implant component or bone structures.
2. Under axial loading, a core/veneer thickness ratio of 5/1 is unfavorable in terms of stress distribution.
3. Under oblique loading, core/veneer thickness ratios of 1/1 and 2/1 are comparatively favorable in terms of stress distribution.

References

1. Guess PC, Schultheis S, Bonfante EA, Coelho PG, Ferencz JL, Silva NR. All-ceramic systems: laboratory and clinical performance. Dent Clin North Am 2011; 55(2): p. 333-52, ix.
2. Ozkurt Z, Kazazoglu E. Clinical success of zirconia in dental applications. J Prosthodont 2010; 19(1): p. 64-8.
3. Silva NR, Sailer I, Zhang Y, Coelho PG, Guess PC, Zembic A, Kohal RJ. Performance of zirconia for dental healthcare. Materials 2010; 3(2): p. 863-896.
4. Larsson C, Wennerberg A. The clinical success of zirconia-based crowns: a systematic review. Int J Prosthodont 2014; 27(1): p. 33-43.
5. Guess PC, Att W, Strub JR. Zirconia in fixed implant prosthodontics. Clin Implant Dent Relat Res 2012; 14(5): p. 633-45.
6. Schwarz S, Schroder C, Hassel A, Bomicke W, Rammelsberg P. Survival and chipping of zirconia-based and metal-ceramic implant-supported single crowns. Clin Implant Dent Relat Res 2012; 14 Suppl 1: p. e119-25.
7. Augstin-Panadero R, Fons-Font A, Roman-Rodriguez JL, Granell-Ruiz M, del Rio-Highsmith J, Sola-Ruiz MF. Zirconia versus metal a preliminary comparative analysis of ceramic veneer behavior. Int J Prosthodont 2012; 25(3): p. 294-300.
8. Zarone F, Russo S, Sorrentino R. From porcelain-fused-to-metal to zirconia: clinical and experimental considerations. Dent Mater 2011; 27(1): p. 83-96.
9. Rosentritt M, Steiger D, Behr M, Handel G, Kolbeck C. Influence of substructure design and spacer settings on the in vitro performance of molar zirconia crowns. J Dent 2009;

37(12): p. 978-83.

10. Larsson C, Madhoun SE, Wennerberg A, Vult von Steyern P. Fracture strength of yttria-stabilized tetragonal zirconia polycrystals crowns with different design: an in vitro study. Clin Oral Implants Res 2012; 23(7): p. 820-6.
11. Sundh A, Sjögren G. A comparison of fracture strength of yttrium oxide partially stabilized zirconia ceramic crowns with varying core thickness shapes and veneer ceramics. J Oral Rehabil 2004; 31(7): p. 682-8.
12. Alhasanyah A, Vaidyanathan TK, Flinton RJ. Effect of core thickness differences on post-fatigue indentation fracture resistance of veneered zirconia crowns. J Prosthodont 2013; 22(5): p. 383-90.
13. Benetti P, Pelogia F, Valandro LF, Bottino MA, Bona AD. The effect of porcelain thickness and surface liner application on the fracture behavior of a ceramic system. Dent Mater 2011; 27(9): p. 948-53.
14. Millen CS, Reuben RL, Ibbetson RJ. The effect of coping/veneer thickness on the fracture toughness and residual stress of implant supported, cement retained zirconia and metal-ceramic crowns. Dent Mater 2012; 28(10): p. e250-8.
15. Lima JM, Souza AC, Anami LC, Bottino MA, Melo RM, Souza RO. Effects of thickness, processing technique, and cooling rate protocol on the flexural strength of a bilayer ceramic system. Dent Mater 2013; 29(10): p. 1063-72.
16. Esquivel-Upshaw JF, Clark AE, Shuster JJ, Anusavice KJ. Randomized clinical trial of implant-supported ceramic-ceramic and metal-ceramic fixed dental prostheses: preliminary results. J Prosthodont 2014; 23(2): p. 73-82.
17. Esquivel-Upshaw JF, Anusavice KJ. Ceramic design concepts based on stress distribution analysis. Compend Contin Educ Dent 2000; 21(8): p. 649-52, 654; quiz 656.
18. Motta AB, Pereira LC, Duda FP, Anusavice KJ. Influence of substructure design and occlusal reduction on the stress distribution in metal ceramic complete crowns: 3D finite element analysis. J Prosthodont 2014; 23(5): p. 381-9.
19. Anami LC, Lima JM, Corazza PH, Yamamoto ET, Bottino MA, Borges AL. Finite element analysis of the influence of geometry and design of zirconia crowns on stress distribution. J Prosthodont 2015; 24(2): p. 146-51.
20. Kirsten A, Parkot D, Raith S, Fischer H. A cusp supporting framework design can decrease critical stresses in veneered molar crowns. Dent Mater 2014; 30(3): p. 321-6.
21. Sung M, Han CH, Kim S. A novel coping design to decrease maximum principal stress in zirconia ceramic restorations. J Prosthodont 2014; 23(7): p. 534-9.
22. Proos K, Steven G, Swain M, Ironside JIM. Preliminary Studies on the Optimum Shape of Dental Bridges. Computer Methods in Biomechanics and Biomedical Engineering 2001; 4(1): p. 77-92.
23. Anusavice KJ, Jadaan OM, Esquivel-Upshaw JF. Time-dependent fracture probability of bilayer, lithium-disilicate-based, glass-ceramic, molar crowns as a function of core/veneer thickness ratio and load orientation. Dent Mater 2013; 29(11): p. 1132-8.
24. Chang CL, Chen CS, Huang CH, Hsu ML. Finite element analysis of the dental implant using a topology optimization method. Med Eng Phys 2012; 34(7): p. 999-1008.
25. Dejak B, Mlotkowski A, Langot C. Three-dimensional finite element analysis of molars with thin-walled prosthetic crowns made of various materials. Dent Mater 2012; 28(4): p. 433-41.
26. Wakabayashi N, Ona M, Suzuki T, Igarashi Y. Nonlinear finite element analyses: advances and challenges in dental applications. J Dent 2008; 36(7): p. 463-71.
27. Murakami N, Wakabayashi N. Finite element contact analysis as a critical technique in dental biomechanics: a review. J Prosthodont Res 2014; 58(2): p. 92-101.
28. Misch CE. Contemporary Implant Dentistry. 3rd ed. 2008.
29. Esquivel-Upshaw JF, Mehler A, Clark AE, Neal D, Anusavice KJ. Fracture analysis of randomized implant-supported fixed dental prostheses. J Dent 2014; 42(10): p. 1335-42.
30. Sotto-Mario BS, Mendes Senna P, da Silva WJ, Rocha EP, Del Bel Cury AA. Influence of crown-to-implant ratio, retention system, restorative material, and occlusal loading on stress concentrations in single short implants. Int J Oral Maxillofac Implants 2012; 27(3): p. e13-8.
31. Rekow ED, Harsono M, Janal M, Thompson VP, Zhang G. Factorial analysis of variables influencing stress in all-ceramic crowns. Dent Mater 2006; 22(2): p. 125-32.
32. Kurtoglu C, Uysal H, Mamedov A. Influence of layer thickness on stress distribution in ceramic-cement-dentin multi-layer systems. Dent Mater J 2008; 27(4): p. 626-32.
33. Wimmer T, Erdelt KJ, Raith S, Schneider JM, Stawarczyk B, Beuer F. Effects of differing thickness and mechanical properties of cement on the stress levels and distributions in a three-unit zirconia fixed prosthesis by FEA. J Prosthodont 2014; 23(5): p. 358-66.
34. Shahrbaf S, vanNoort R, Mirzakouchaki B, Ghassemieh E, Martin N. Effect of the crown design and interface lute parameters on the stress-state of a machined crown-tooth system: a finite element analysis. Dent Mater 2013; 29(8): p. e123-31.
35. Swain MV. Unstable cracking (chipping) of veneering porcelain on all-ceramic dental crowns and fixed partial dentures. Acta Biomater 2009; 5(5): p. 1668-77.
36. Guazzato M, Walton TR, Franklin W, Davis G, Bohl C, Klineberg I. Influence of thickness and cooling rate on development of spontaneous cracks in porcelain/zirconia structures. Aust Dent J 2010; 55(3): p. 306-10.
37. Benetti P, Kelly JR, Sanchez M, Della Bona A. Influence of thermal gradients on stress state of veneered restorations. Dent Mater 2014; 30(5): p. 554-63.
38. Zhang Z, Guazzato M, Sornsuwan T, Scherrer SS, Rungsiyakull C, Li W, Swain MV, Li Q. Thermally induced fracture for core-veneered dental ceramic structures. Acta Biomater 2013; 9(9): p. 8394-402.